

# Monte Carlo - Optimization Design of Concentrating Mirror Field for Clustering Algorithm

Kunyang Zhou\*, Xiaotong Wang

School of International Education, Neusoft Institute, Foshan 528225, Guangdong, China

*\*Author to whom correspondence should be addressed.*

**Copyright:** © 2026 Author(s). This is an open-access article distributed under the terms of the Creative Commons Attribution License (CC BY 4.0), permitting distribution and reproduction in any medium, provided the original work is cited.

**Abstract:** Tower solar thermal power is a high-efficiency clean energy source. Aiming at low optical efficiency and unreasonable layout in the heliostat field, this paper proposes an integrated optimization method combining Monte-Carlo ray tracing and DBSCAN clustering. The optical efficiency model is established to calculate the cosine, shading, atmospheric and truncation efficiency. On this basis, the tower position, heliostat size, height and layout are optimized. Results show that the proposed method significantly improves the annual average thermal power output per unit area. This design provides an effective solution for engineering applications. Due to the optimized layout allowing more heliostats to be deployed within the same footprint, the total power output has nearly doubled. The annual average output thermal power increases from 32.40 MW to 65.59 MW, and the annual average output thermal power per unit mirror area increases from 0.516 kW/m<sup>2</sup> to 0.690 kW/m<sup>2</sup>.

**Keywords:** Monte-Carlo algorithm; DBSCAN clustering; Heliostat field layout; Optical efficiency; Output thermal power

**Online publication:** March 26, 2026

## 1. Introduction

Under the background of global energy transformation and low-carbon development, solar energy plays an increasingly important role in the clean energy system. Tower solar thermal power generation is widely used due to its high efficiency and good stability. The heliostat field is the key subsystem that affects the energy output of the whole power station. At present, most heliostat field designs have shortcomings such as low optical efficiency, serious shadow loss, and inefficient layout algorithms, which restrict the improvement of system performance. In order to solve these problems, this paper focuses on the optimal design of heliostat field based on Monte-Carlo and clustering algorithm, aiming to improve energy output efficiency and provide a reliable scheme for practical engineering <sup>[1]</sup>.

## 2. Optical efficiency calculation formulas

### 2.1. Solar hour angle calculation

The solar hour angle indicates the position of the sun relative to the local noon. The calculation formula is derived based on the difference between local time and noon.

$$\omega_m = \frac{\pi}{12}(ST_m - 12)$$

Among them,  $\omega_m$  represents the solar hour angle at the  $m$ th moment (unit: rad); represents the local time at the  $m$ th moment (unit: h), with values of 9, 10.5, 12, 13.5, and 15, is the mathematical constant  $\pi$  (approximately 3.1416).

## 2.2. Solar declination angle

The solar declination angle describes the latitude of the Sun's direct rays, varying sinusoidally over the year. Taking the vernal equinox (March 21) as day 0, it is calculated as:

$$\sin \delta_m = \sin\left(\frac{2\pi}{365}\right) \cdot \sin\left(\frac{2\pi \times 23.45}{365}\right) \quad (1)$$

$\delta_m$ : solar declination at the  $m$ -th moment (rad); 23.45°: obliquity of the ecliptic.

## 2.3. Solar altitude angle calculation

The solar altitude angle is the angle between the sun's rays and the horizontal plane, which determines the incident angle of solar radiation. The formula comprehensively considers the effects of solar declination, local latitude, and solar hour angle, with a range of 0°–90°.

$$\sin \alpha_{s,m} = \cos \delta_m \cos \varphi \cos \omega_m + \sin \delta_m \sin \varphi \quad (2)$$

## 2.4. Monthly average optical efficiency calculation

The monthly average optical efficiency is defined as the average of the total optical efficiencies of all heliostats at all calculation times within the month. It reflects the monthly average optical performance of the heliostat field.

$$\bar{\eta}_{month} = \frac{1}{M} \sum_{i=1}^{N_0} \sum_{m=1}^M \eta_{i,m} \quad (3)$$

$\bar{\eta}_{month}$  represents the monthly average optical efficiency of the heliostat field;  $M$  is the number of calculation times per month (with  $M = 5$  as five representative times are selected each month);  $N_0$  is the total number of heliostats;  $\eta_{i,m}$  is the optical efficiency of the  $i$ th heliostat at the  $m$ th time step.

## 2.5. Annual average output thermal power per unit mirror area calculation

The power per unit area is the ratio of the annual average total power to the total mirror field area. It reflects the energy utilization efficiency of the mirrors and is one of the key indicators for evaluating the performance of a heliostat field design.

$$P_{avg} = \frac{E_{field,avg} \times 1000}{\sum_{i=1}^{N_0} A_i} \quad (4)$$

$E_{field,avg}$  represents the annual average output thermal power per unit mirror area (unit: kW/m<sup>2</sup>);  $P_{avg}$  represents the annual average output thermal power (unit: MW), Multiplying by 1000 converts MW to kW;  $\sum_{i=1}^{N_0} A_i$  is the total area of the heliostat field.

## 2.6. Monthly average cosine efficiency

The monthly average cosine efficiency reflects the impact of the solar incident angle relative to the mirror normal on monthly energy collection, calculated as:

$$\bar{\eta}_{\cos,month} = \frac{1}{M} \sum_{i=1}^{N_0} \sum_{m=1}^M \eta_{\cos,i,m} \quad (5)$$

where  $\bar{\eta}_{\cos,month}$  is the field-level average, and  $\eta_{\cos,i,m}$  is the instantaneous cosine efficiency of heliostat  $i$  at time  $m$  (equal to  $\sin \alpha_{s,m}$  under ideal tracking).

### 2.7. Monthly average shading and blocking efficiency

The monthly average shading and blocking efficiency quantifies energy losses due to tower and inter-heliostat obstruction, calculated as:

$$\bar{\eta}_{sb,month} = \sum_{i=1}^{N_0} \sum_{m=1}^M \eta_{sb,i,m} \quad (6)$$

where  $\eta_{sb,i,m}$  is the field-level average, and  $\eta_{sb,i,m}$  is the instantaneous efficiency of heliostat  $i$  at time  $m$  (equal to  $1 - \text{total shading/blocking loss}$ ).

### 2.8. Monthly average truncation efficiency

The monthly average truncation efficiency quantifies the effective energy utilization resulting from the validity of the projected light cone, calculated as:

$$\bar{\eta}_{trunc,month} = \frac{1}{M} \sum_{i=1}^{N_0} \sum_{m=1}^M \eta_{trunc,i,m} \quad (7)$$

where  $\bar{\eta}_{trunc,month}$  is the field-level average, and  $\eta_{trunc,i,m}$  is the instantaneous truncation efficiency of heliostat  $i$  at time  $m$ , computed via ray tracing as:

$$\eta_{trunc,i,m} = \frac{N_{valid,i,m}}{N_{RAYS}} \quad (8)$$

### 2.9. Regional optical efficiency analysis

The heliostat field is partitioned into 100 regions. Mean optical efficiency for each region is obtained by averaging all heliostat efficiencies at each time step, and the results are presented as an average optical efficiency heatmap.

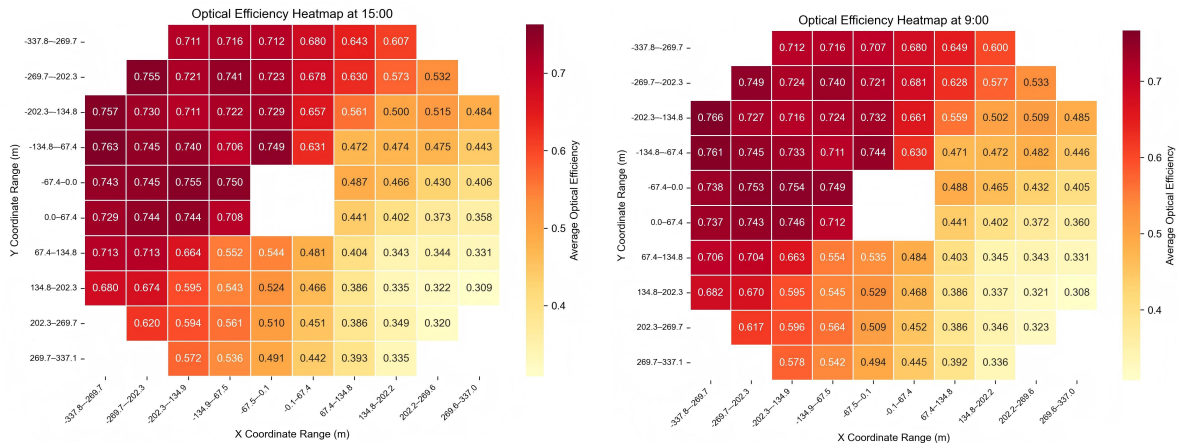


Figure 1. Regional average optical efficiency heatmaps.

### 3. Algorithm and design

To determine the optimal layout direction based on the efficiency distribution, the entire heliostat field is first divided into small regions, and the direction with the strongest optical efficiency is identified. For this purpose, we select the region with an average optical efficiency greater than 70% and perform a linear fit to guide the arrangement of more heliostats in this high-efficiency direction, making the design more scientific and effective. The fitting result, which yields the following equation, is validated by an  $R^2$  of 0.98 and an RMSE of 0.025, confirming its reliability in reflecting the high-efficiency trend:

Fitted Equation:

$$y = -0.457878x - 208.521521 \quad (9)$$

The receiver tower coordinates are (227.3054, -104.0781), obtained by moving 100 m along the fitted line from its intersection with the circular boundary. Accordingly, all heliostats are arranged within the region enclosed by this large circular boundary. Then, the positions and heights of the tracking mirrors are initialized according to the circular trajectory.

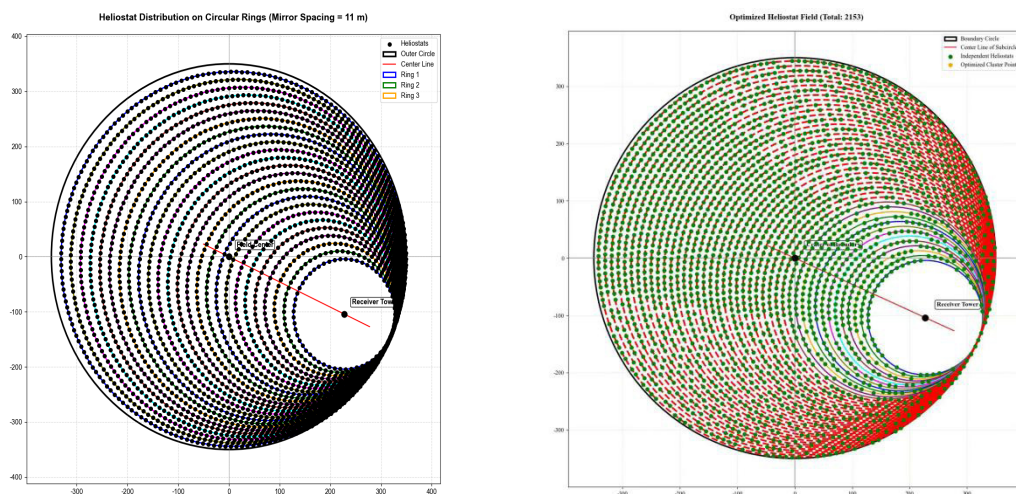


Figure 2. Algorithm effect diagram.

First, for Monte Carlo - for clustering algorithms preparation and receiver siting, heliostats with average optical efficiency above 0.7 at four typical times are screened and linearly fitted to determine the optimal layout direction, and the receiver position is then optimized along the reverse direction. Second, heliostats are arranged along circular arcs with an initial interval of 5 m between heliostats and variable arc spacing, and arc generation stops when exceeding the construction boundary <sup>[2]</sup>.

Finally, DBSCAN spatial clustering is adopted to avoid the high time complexity of exhaustive methods: taking the 2D planar coordinates  $(x,y)$  of all initialized heliostats as input features, with parameters set as  $\text{eps} = \text{mirror width} + 5\text{m}$  and  $\text{min\_samples} = 2$ , the algorithm automatically identifies dense heliostat clusters and independent noise points. Each identified dense cluster is then processed by the Monte Carlo optimization algorithm: mirrors in the cluster are randomly shuffled, and only those maintaining the minimum safe distance from all previously retained mirrors are kept. This random selection process is repeated 50 times to obtain the optimal solution that retains the maximum number of valid mirrors while satisfying the spacing constraint. In this way, dense heliostat groups are iteratively adjusted until all inter-heliostat distances meet the spacing constraint of mirror width plus 5 m.

## 4. Designed performance

### 4.1. Overall design improvement effect

The optimization significantly improved the overall system performance. After optimization, the annual average optical efficiency increased by 2.93%, the total thermal power output rose by 102.40%, and the specific thermal power per mirror area increased by 33.71%. These results demonstrate that the proposed layout and receiver positioning strategy effectively improve energy utilization efficiency and comprehensive power generation capacity<sup>[3]</sup>.

**Table 1.** Gesture correspondence table

	Annual Average Optical Efficiency	Annual Average Cosine Efficiency	Annual Average Shading & Blocking Efficiency	Annual Average Truncation Efficiency	Annual Average Thermal Power Output (MW)	Annual Average Thermal Power Output per Unit Mirror Area (kW/m <sup>2</sup> )
Before Optimization	0.597440	0.759788	0.967854	0.899977	32.40369	0.515818
After Optimization	0.61493	0.774332	0.942904	0.919942	65.586292	0.689699
Growth Rate	0.029274	0.019142	-0.0257786	0.022183	1.024037	0.337098

### 4.2. 3D optimized heliostat layout with efficiency mapping

The diurnal optical efficiency distribution shows that the optimized heliostat field maintains high and stable efficiency at different times of the day. The efficiency distribution is uniform without obvious attenuation, which verifies that the layout can adapt to the change of solar position and maintain good optical performance throughout the whole day.

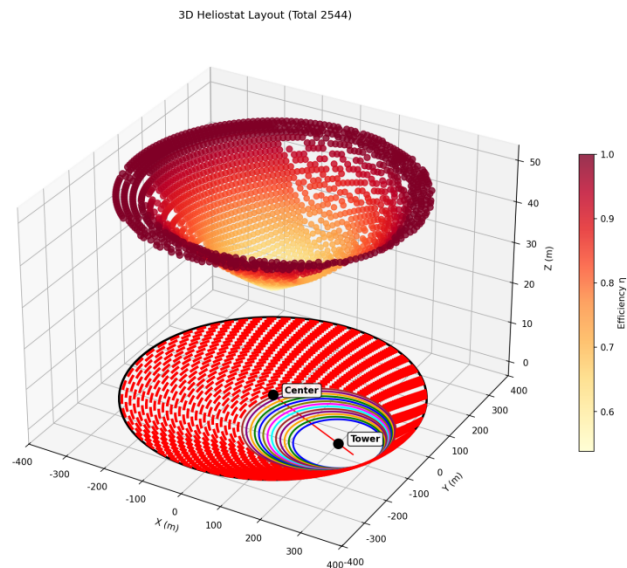


**Figure 3.** Optimized heliostat layout with efficiency mapping.

### 4.3. Diurnal optical efficiency distribution

The optimization significantly improved the system performance, as shown in the efficiency metrics, 3D layout, and diurnal distribution results: due to the optimized layout allowing more heliostats to be deployed within the same footprint, the total thermal power output rose dramatically by 102.40%, while the annual average optical efficiency increased by 2.93% and the specific thermal power per mirror area improved by 33.71%, respectively. These improvements, supported by consistent high-efficiency distributions across different times of day and the optimized 3D heliostat arrangement,

confirm that the proposed layout and receiver positioning strategy effectively enhance energy utilization efficiency and overall power generation capability [4].

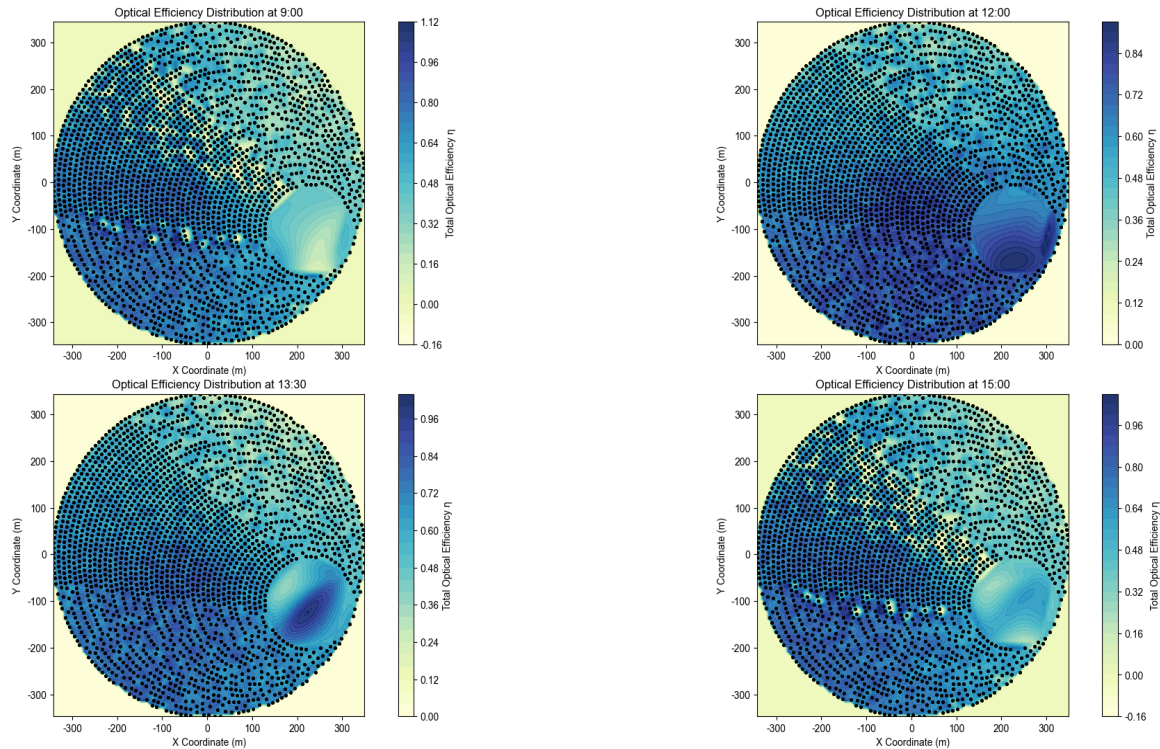


Figure 4. Diurnal optical efficiency distribution.

## 5. Conclusion

This work presents an optimized heliostat field layout strategy using a clustering-based ray-tracing algorithm to enhance both optical efficiency and thermal performance. The proposed algorithm efficiently reduces computational complexity while optimizing receiver positioning and heliostat arrangement, resulting in a 2.93% increase in annual average optical efficiency, a 102.40% rise in total thermal power output, and a 33.71% improvement in specific power per mirror area. Diurnal efficiency maps confirm stable, high-performance operation across different times of day, and the design satisfies all geometric constraints while effectively balancing shading and truncation effects, offering an efficient and practical solution for tower solar power plants.

## Disclosure statement

The authors declare no conflict of interest.

## References

- [1] Yang G, 2022, Influence of Solar Shape and Optical Errors on Focused Energy Spillage in Tower Solar Thermal Power Plants, thesis, North China Electric Power University (Beijing).
- [2] Liu R, Yu Y, Liu J, et al., 2025, Electric Vehicle Charging Load Prediction Based on Improved Monte Carlo Algorithm. *Zhejiang Electric Power*, 44(8): 15–23.

- 
- [3] Han S, Yang N, Yao Y, et al., 2025, Derivation of Rain Patterns in Jiangsu Province Based on Cluster Analysis. *Journal of Hydrology*, 46(1): 91–97.
- [4] Qian W, Lu X, Yun T, et al., 2025, A Ray-Tracing Algorithm Based on Discrete Anisotropic Radiative Transfer Model. *Journal of Northwest Forestry University*, 40(1): 1–10.

**Publisher's note**

*Whoice Publishing remains neutral with regard to jurisdictional claims in published maps and institutional affiliations.*